

# Leader-follower Based Target Detection Model for Mobile Molecular Communication Networks

Tadashi Nakano<sup>1</sup>, Shouhei Kobayashi<sup>2</sup>, Takako Koujin<sup>2</sup>, Chen-Hao Chan<sup>3</sup>, Yu-Hsiang Hsu<sup>3</sup>,  
Yutaka Okaie<sup>1</sup>, Takuya Obuchi<sup>4</sup>, Takahiro Hara<sup>4</sup>, Yasushi Hiraoka<sup>1,2</sup>, Tokuko Haraguchi<sup>2</sup>

<sup>1</sup>Graduate School of Frontier Biosciences, Osaka University, Japan

<sup>2</sup>National Institute of Information and Communications Technology, Japan

<sup>3</sup>Institute of Applied Mechanics, National Taiwan University, Taiwan

<sup>4</sup>Graduate School of Information Science and Technology, Osaka University, Japan

Email: tadasi.nakano@fbs.osaka-u.ac.jp

**Abstract**—This paper proposes a leader-follower based target detection model for mobile molecular communication networks. The proposed model divides application functionalities of molecular communication networks over the two types of mobile bio-nanomachine: leader and follower bio-nanomachines. Leader bio-nanomachines distribute in the environment to detect a target and create an attractant gradient around the target. Follower bio-nanomachines move based on the attractant gradient made by leader bio-nanomachines, approach the target and perform necessary functionalities such as releasing drug molecules. The functional division demonstrated through the model facilitates the design and development of molecular communication networks as it can reduce the number of functionalities that need to be implemented on individual bio-nanomachines.

**Index Terms**—Molecular communication, mobile bio-nanomachine, leader-follower model, target detection

## I. INTRODUCTION

Molecular communication networks or collections of bio-nanomachines that communicate through molecular communication are expected to perform complex functionalities within biological systems [1], [2], [3], [4]. Example applications of such networks include transporting drug molecules to target locations (e.g., disease sites) [5], [6], releasing drug molecules at target locations [7], [8], [9], and tracking the locations of mobile targets inside the human body [10], [11].

This paper describes a leader-follower based target detection model for mobile molecular communication networks. The leader-follower model proposed in this paper divides key functionalities of mobile molecular communication networks to perform target detection over the two types of mobile bio-nanomachine: leader and follower bio-nanomachines. Leader bio-nanomachines distribute in the environment to detect a target. Upon detecting a target, leader bio-nanomachines start releasing an attractant molecule, creating an attractant gradient around the target. Follower bio-nanomachines move based on the attractant gradient made by leader bio-nanomachines, approach the target, and perform necessary functionalities such as releasing drug molecules.

The main contributions of this paper include developing a new model of mobile molecular communication networks for target detection application. The functional division demon-

strated in this model facilitates the design and development of bio-nanomachines as it can reduce the number of functionalities that need to be implemented by individual bio-nanomachines. The main contributions of this paper also include mathematical modeling and a feasibility study that combines wet laboratory experiments and computer simulations to demonstrate target detection capabilities of the proposed model.

The rest of the paper is organized as follows. Section II introduces briefly the leader-follower based target detection model that we propose in this paper. Section III mathematically defines the proposed model and Section IV describes our feasibility study to demonstrate the potential of the proposed model to perform target detection. Finally, Section V summarizes this work to conclude the paper.

## II. OVERVIEW

This paper proposes a leader-follower based target detection model of mobile molecular communication networks (i.e., collections of mobile bio-nanomachines). Target detection is a key functionality of mobile molecular communication networks [10], [12], [13]. Target detection considered in this paper consists of (1) distributing mobile bio-nanomachines in the environment, (2) identifying the location of a target in the environment, and (3) directing bio-nanomachines to the target location where they perform collective actions (such as releasing drug molecules).

This section first describes our assumptions for and examples of key components that constitute the target detection application considered in this paper: the monitoring environment, targets, bio-nanomachines and molecular communication networks. This section then introduces the leader-follower based target detection model of mobile molecular communication networks.

### A. Key Components

Target detection is performed in the environment of interest, referred to as the **monitoring environment**. The monitoring environment is an aqueous and small-scale environment (e.g., up to tens of mm). It may contain molecules and energy

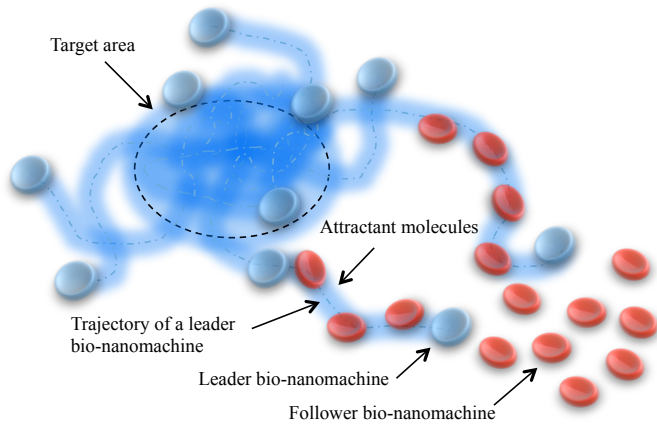


Fig. 1. Leader-follower based mobile molecular communication network for target detection

sources for bio-nanomachines to perform necessary functionalities. It may also contain noise sources such as thermal noise and other molecules (noise molecules) that may interfere with functionalities of bio-nanomachines. An example of the monitoring environment is the internal environment of the human body.

**Targets** are biochemical objects that appear in the monitoring environment. Targets are assumed to be chemically identifiable. For instance, targets may express specific proteins on their surface, and bio-nanomachines may physically contact the surface receptors to identify the targets. Targets may also secrete diffusive marker molecules and bio-nanomachines may detect the marker molecules to learn the presence of targets. Examples of targets include diseased cells and tissues.

A **bio-nanomachine** is defined based on three criteria: material, size and functionality [14]. A bio-nanomachine is composed of biomaterials (e.g., proteins, nucleic acids, lipids, biological cells) with or without non-biomaterials (e.g., magnetic particles and gold nanorods) [15]. The size of a bio-nanomachine ranges from the size of a macromolecule to that of a biological cell (i.e., dimensions of 1 – 100  $\mu\text{m}$ ). A bio-nanomachine implements a set of simple functionalities to manipulate molecules, such as detecting, modifying and releasing molecules. A bio-nanomachine may have mobility, an ability to produce directional motion in the monitoring environment; such bio-nanomachines are called *mobile* bio-nanomachines. Examples of bio-nanomachines include genetically modified cells and artificially engineered cells.

Bio-nanomachines communicate through molecular communication to form a **molecular communication network**. Two types of molecular communication are considered: diffusion-based and non-diffusion-based molecular communication. In diffusion-based molecular communication, bio-nanomachines communicate by propagating diffusive molecules in the environment [12]. In non-diffusion-based molecular communication, bio-nanomachines communicate by using adhesive molecules [13]. In this paper, molecular com-

munication networks that consist of mobile bio-nanomachines are referred to as *mobile* molecular communication networks.

### B. Leader-follower Based Target Detection Model

The leader-follower based target detection model proposed in this paper assumes two types of mobile bio-nanomachine, leader and follower bio-nanomachines that cooperate to perform target detection (Fig. 1).

- Leader bio-nanomachines distribute in the environment to detect a target. Upon detecting a target, leader bio-nanomachines start releasing attractant molecules while they continue to move in the environment.
- Follower bio-nanomachines move in the environment and detect an attractant molecule. In the presence of attractant molecules, follower bio-nanomachines move preferentially to the higher attractant concentration. Follower bio-nanomachines implement application-dependent functionalities. For example, in drug delivery applications (i.e., delivery of drug molecules to target cancer cells), they may carry drug molecules that need to be released at target locations.

The proposed model uses an adhesive type of attractant molecule; namely, bio-nanomachines use non-diffusion-based molecular communication. Attractant molecules released by leader bio-nanomachines bind to the surface of an environment and remain where they are released. As shown in Fig. 1, the attractant molecules may form a trail as a leader bio-nanomachine moves in the environment. When the attractant trail forms a loop that includes the target location, follower bio-nanomachines following the trail may reach the target. Using adhesive molecules has several advantages over using diffusive molecules [13]; for example, the attractant concentration remains high for a long period of time (because the attractant molecules do not diffuse away) allowing bio-nanomachines to detect the concentration.

## III. LEADER-FOLLOWER BASED TARGET DETECTION MODEL

This section describes the leader-follower based target detection model proposed in this paper. For simplicity, this section assumes the following:

- The monitoring environment is two-dimensional and defined as an area  $A$ .
- The target exists uniformly in a sub-area  $A_T (\subseteq A)$  within the monitoring environment.
- Bio-nanomachines do not physically interact with each other. They move in the two-dimensional monitoring area independently from each other.

### A. Leader Bio-nanomachines

We use the Langevin equation to describe the mobility of a leader bio-nanomachine. The Langevin equation originally describes Brownian motion of a particle in a fluid medium; here it is applied to model the mobility of a bio-nanomachine.

Let  $S_l$  denote a set of leader bio-nanomachines. For each leader bio-nanomachine  $i \in S_l$ , we have

## IV. FEASIBILITY STUDY

$$\frac{d^2 \vec{X}_i(t)}{dt^2} = -\alpha \frac{d\vec{X}_i(t)}{dt} + \beta \frac{d\vec{W}(t)}{dt}, \quad (1)$$

where  $\vec{X}_i(t)$  is the location of leader bio-nanomachine  $i$  at time  $t$ ,  $\alpha$  is a positive constant determining the resistance to the bio-nanomachine's motion,  $\beta$  is a positive constant determining the degree of noise effects on the bio-nanomachine's motion, and  $\vec{W}(t)$  is the Wiener process (noise effects).

A leader bio-nanomachine is either releasing  $M(> 0)$  attractant molecules (per unit time) or not releasing attractant molecules according to the following rules:

- Leader bio-nanomachine  $i$  ( $\in S_l$ ) in the target area ( $\vec{X}_i(t) \in A_T$ ) releases attractant molecules.
- Leader bio-nanomachine  $i$  ( $\in S_l$ ) outside the target area ( $\vec{X}_i(t) \notin A_T$ ) releases attractant molecules if it recently visited the target area, namely, if the time elapsed since its most recent visit to the target area is within the attractant release time duration  $T$ . Leader bio-nanomachine  $i$  does not release attractant molecules if it never visited the target area.

### B. Attractant Concentration

Attractant molecules released by leader bio-nanomachines remain where they are released. Attractant molecules do not diffuse as they are assumed to be adhesive and bind to the surface of the monitoring environment. Attractant molecules in the environment decay with time. Let  $c(\vec{x}, t)$  denote the surface concentration of attractant molecule at location  $\vec{x}$  and time  $t$ . Then the rate of change in  $c(\vec{x}, t)$  is given by a partial differential equation:

$$\frac{\partial c(\vec{x}, t)}{\partial t} = \sum_{i \in S_a(t)} M \delta(\vec{x} - \vec{X}_i(t)) - kc(\vec{x}, t), \quad (2)$$

where  $S_a(t)$  is the set of active leader bio-nanomachines at time  $t$ ,  $\delta(\cdot)$  is the Dirac delta function expressing the locations where leader bio-nanomachines release attractant molecules, and  $k$  is the degradation rate constant of the attractant molecule.

### C. Follower Bio-nanomachines

We also use the Langevin equation to describe the mobility of a follower bio-nanomachine. Let  $S_f$  denote a set of follower bio-nanomachines. For each follower bio-nanomachine  $i \in S_f$ , we have

$$\frac{d^2 \vec{X}_i(t)}{dt^2} = -\alpha \frac{d\vec{X}_i(t)}{dt} + \beta \frac{d\vec{W}(t)}{dt} + \gamma \nabla c(\vec{x}, t)|_{\vec{x}=\vec{X}_i(t)}, \quad (3)$$

where  $\gamma$  is a positive constant determining the impact of the attractant concentration gradient  $\nabla c(\vec{x}, t)$  at location  $\vec{x} = \vec{X}_i(t)$  on the directional motion of the bio-nanomachine and  $\nabla = \vec{e}_x \frac{\partial}{\partial x} + \vec{e}_y \frac{\partial}{\partial y}$ .

This section describes our feasibility study to demonstrate that the leader and follower bio-nanomachines defined in Section III collectively perform target detection. The feasibility study consists of (1) wet-laboratory experiments to estimate model parameters and (2) computer simulations in which estimated parameter values are used to demonstrate the collective behavior of leader and follower bio-nanomachines to perform target detection.

#### A. Parameter Estimation

We first performed wet laboratory experiments to identify key parameters  $\alpha$ ,  $\beta$ , and  $\gamma$  in (1) and (3). In wet laboratory experiments, we used endothelial cells as a model of bio-nanomachines since they are known to produce directional motion [16]. We also used fibronectin as an attractant molecule since endothelial cells appear to move up the fibronectin gradient [17], [18].

We performed two sets of experiments. In the first set of experiments (control experiments), we spread cells on a glass surface without fibronectin and fibronectin gradients. In the second set of experiments, we spread cells on a gradient surface where the fibronectin concentration increases linearly along a direction on the surface. In both sets of experiments, we tracked locations of cells every 10 min over 12 hours. Figs. 2A-C show representative trajectories of selected cells: Fig. 2A from the first set of experiments and Figs. 2B and C from the second set of experiments.

Each trajectory of a cell is given as a sequence of the cell's locations on a two-dimensional surface:  $(x_i, y_i)$  with  $i = 0, 1, \dots, 72$ . (The cell's location was measured every 10 min over 12 hours, yielding a sequence of 73 locations.) Given a trajectory, we used the maximum likelihood estimation (MLE) to estimate  $\alpha$ ,  $\beta$ ,  $\gamma$ . Briefly, we first rewrote (3) as

$$\frac{d^2 X(t)}{dt^2} = -\alpha \frac{dX(t)}{dt} + \beta \frac{dW_x(t)}{dt} + \gamma', \quad (4)$$

$$\frac{d^2 Y(t)}{dt^2} = -\alpha \frac{dY(t)}{dt} + \beta \frac{dW_y(t)}{dt}, \quad (5)$$

where the fibronectin gradient is assumed to be made along the x-axis and  $\gamma'$  determines the directional force that moves cells along the axis:  $\gamma' = \gamma \frac{\partial c}{\partial x}$  where  $\frac{\partial c}{\partial x}$  is a constant since the gradient is linear.

We then used the MLE method to estimate the parameter values  $\alpha$ ,  $\beta$ ,  $\gamma'$ . For each location  $(x_i, y_i)$  ( $i = 1, 2, \dots$ ), we used (4) and (5) to describe the probability  $P_i$  that the cell moves from  $(x_i, y_i)$  to its next location  $(x_{i+1}, y_{i+1})$ . We then found parameter values  $\alpha$ ,  $\beta$ ,  $\gamma'$  that can maximize the likelihood function ( $\prod_{i=1}^{72} P_i$ ). We also estimated the value of  $\gamma$  based on the relationship  $\gamma' = \gamma \frac{\partial c}{\partial x}$  and an experimentally measured value of  $\frac{\partial c}{\partial x} = 0.02$  (AU/ $\mu\text{m}$ ).

The MLE method is applied to the trajectories shown in Figs. 2A-C and parameter values are estimated (Table I). Note that, for the trajectory shown in Fig. 2A, we used  $\gamma' = 0$  since no fibronectin gradient was formed on the substrate used in the experiment. Further, these parameter values are used

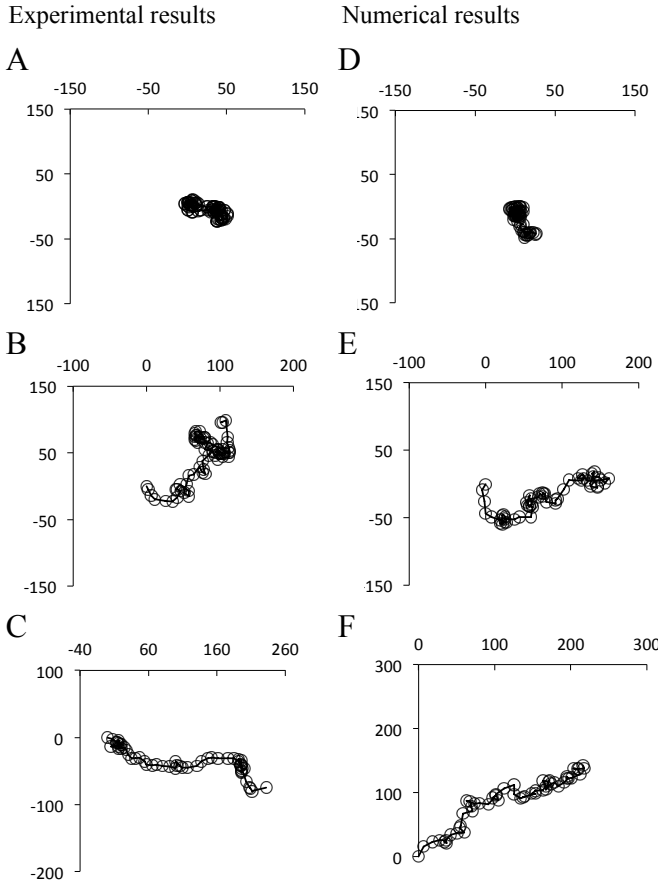


Fig. 2. Trajectories of cells that moved on a non-gradient substrate (A) or gradient substrate (B and C), each obtained from 12 hours of time-lapse imaging. On a gradient substrate, the fibronectin concentration increases from left to right. The cell's starting position is the origin of the two-dimensional coordinate. Parameter values estimated from trajectories A-C are used to produce trajectories D-F. Axis unit is  $\mu\text{m}$ .

TABLE I  
ESTIMATED PARAMETER VALUES

Trajectory shown in	$\alpha$	$\beta$	$\gamma'$	$\gamma$
Fig. 2A	0.097	0.001	–	–
Fig. 2B	0.067	0.019	0.011	0.55
Fig. 2C	0.095	0.020	0.042	2.1

in (4) and (5) to produce trajectories in silico. Figs. 2D-F show examples of reproduced trajectories: Fig. 2D is based on parameter values estimated from the trajectory in Fig. 2A, Fig. 2E from Fig. 2B, and Fig. 2F from Fig. 2C.

### B. Simulation Configurations

For computer simulations, we chose  $\alpha = 0.067$ ,  $\beta = 0.019$ ,  $\gamma = 0.55$  in Table I. Other parameters are determined arbitrary:  $M = 1$ ,  $T = 10^4$ , and  $k = 10^{-6}$ . The simulation environment is also configured arbitrary as follows:

- The monitoring environment is defined as  $A = \{(x, y) | -\frac{L}{2} \leq x \leq \frac{L}{2}, -\frac{L}{2} \leq y \leq \frac{L}{2}\}$  with  $L = 1$  (cm). It is then divided into  $100 \times 100$  ( $\mu\text{m}^2$ ) square areas to solve (2).

- The target area is defined as  $A_T = \{(x, y) | -\frac{L_T}{2} \leq x \leq \frac{L_T}{2}, -\frac{L_T}{2} \leq y \leq \frac{L_T}{2}\}$  with  $L_T = 100$  ( $\mu\text{m}$ ).

At time  $t = 0$ , 100 leader bio-nanomachines and 100 follower bio-nanomachines are placed all at the same location  $(x, y) = (-d, 0)$  with  $d = 1000$  ( $\mu\text{m}$ ). All these bio-nanomachines have zero moving velocity at  $t = 0$  and move based on (1) or (3) for  $t > 0$ . Bio-nanomachines are not allowed to move outside the monitoring environment; they bounce back when they hit the boundaries.

### C. Simulation Results

Fig. 3 shows how the attractant concentration, leader bio-nanomachine distribution and follower bio-nanomachine distribution evolve with time. As shown in the series of images (top), leader bio-nanomachines distribute in the environment, and eventually they become relatively uniformly distributed in the environment (at  $t = 165$  hours). The target area is defined as the square area in the top left image in Fig. 3, and leader bio-nanomachines that enter this area start releasing attractant molecules. The leader bio-nanomachines releasing attractant molecules continue to move in the environment, leading to the formation of attractant concentration gradients as shown in the series of images (middle). Since attractant molecules assumed in this paper are adhesive and not diffusive, the attractant concentration tends to form trails; see the attractant concentrations at  $t = 35$  and  $85$  (hours). As more leader bio-nanomachines release attractant molecules and move in the environment, the attractant gradient is formed. The attractant concentration is high at the target area and it tends to decrease as the distance from the target area increases. This formation of the attractant concentration gradient allows follower bio-nanomachines to move closer to the target area. As shown in the series of images (bottom), follower bio-nanomachines are gradually attracted to the target area.

## V. CONCLUSION

This paper described a leader-follower based target detection model for mobile molecular communication networks. The main advantage of this model is to divide key functionalities of mobile molecular communication networks over two types of bio-nanomachines. This paper also described mathematical models to examine the behavior of the leader-follower based model. It further described wet laboratory experiments to estimate the parameter values for the mathematical models, and demonstrated through computer simulations the collective behavior of leader and follower bio-nanomachines to perform target detection.

Both modeling and experimental studies described in this paper are preliminary. We plan to perform more realistic modeling and an extensive set of experiments to investigate the feasibility of the leader-follower based target detection model that we proposed in this paper.

### ACKNOWLEDGMENTS

This work was supported in part by the Japan Society for the Promotion of Science (JSPS) through the Grant-in-Aid for

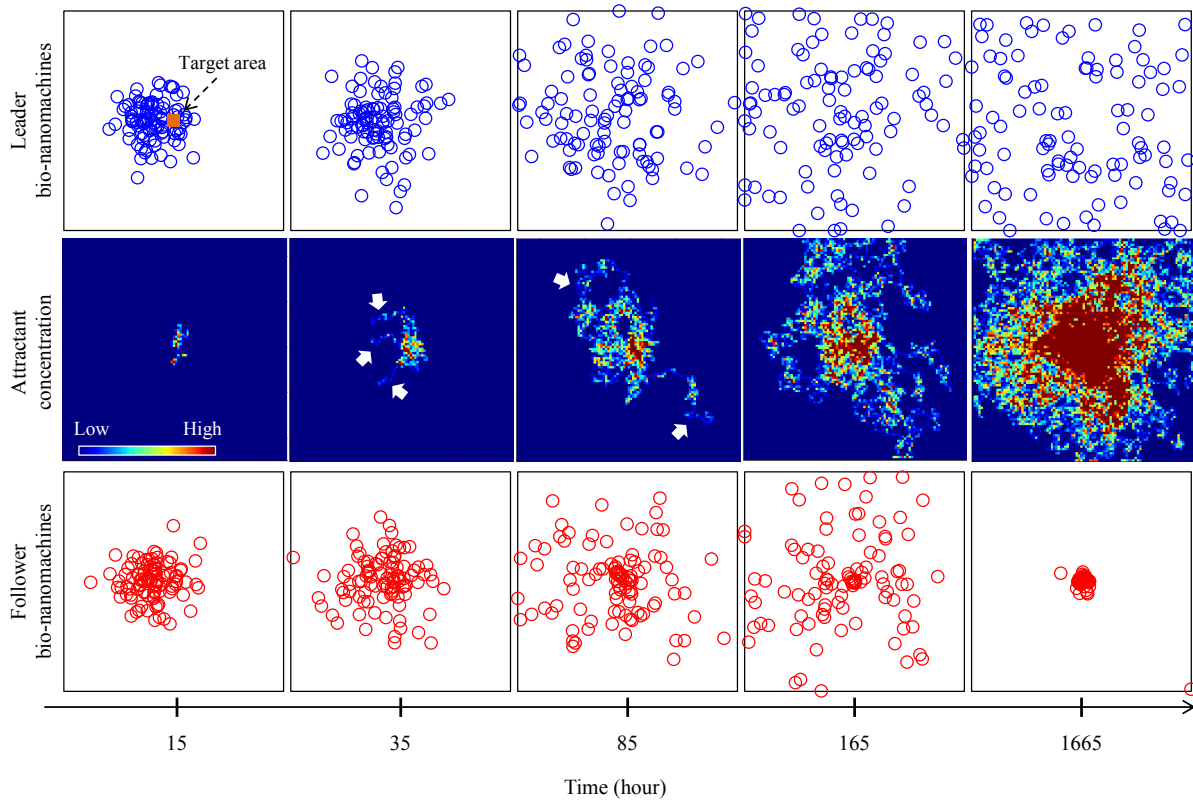


Fig. 3. Leader bio-nanomachine distribution (top), attractant concentration (middle), and follower bio-nanomachine distribution (bottom). Each image shows the  $1 \text{ (cm)} \times 1 \text{ (cm)}$  monitoring area. The target area is  $100 \text{ (}\mu\text{m)} \times 100 \text{ (}\mu\text{m)}$  at the center of the monitoring area as shown in the top left image. Leader and follower bio-nanomachines are represented by circles. The attractant concentration is indicated by the color code. Arrows in attractant concentration point to attractant trails.

Scientific Research (No. 25240011) and the Leading Graduate School Programs.

#### REFERENCES

- [1] I. F. Akyildiz, F. Brunetti, and C. Blazquez, "Nanonetworks: a new communication paradigm," *Computer Networks*, vol. 52, no. 12, pp. 2260–2279, 2008.
- [2] S. Hiyama and Y. Moritani, "Molecular communication: harnessing biochemical materials to engineer biomimetic communication systems," *Nano Communication Networks*, vol. 1, no. 1, pp. 20–30, 2010.
- [3] T. Nakano, M. Moore, F. Wei, A. V. Vasilakos, and J. W. Shuai, "Molecular communication and networking: opportunities and challenges," *IEEE Transactions on NanoBioscience*, vol. 11, no. 2, pp. 135–148, 2012.
- [4] T. Nakano, A. Eckford, and T. Haraguchi, *Molecular Communication*. Cambridge University Press, 2013.
- [5] G. Wei, P. Bogdan, and R. Marculescu, "Bumpy rides: Modeling the dynamics of chemotactic interacting bacteria," *IEEE Journal of Selected Areas in Communication (JSAC)*, vol. 31, no. 12, pp. 879–890, 2013.
- [6] N. R. Raz, M.-R. Akbarzadeh-T., and M. Tafaghodi, "Bioinspired nanonetworks for targeted cancer drug delivery," *IEEE Transactions on NanoBioscience*, vol. 14, no. 8, pp. 894–906, 2015.
- [7] L. Felicetti, M. Femminella, G. Reali, T. Nakano, and A. V. Vasilakos, "TCP-like molecular communications," *IEEE Journal of Selected Areas in Communication (JSAC)*, vol. 32, no. 12, pp. 2354–2367, 2014.
- [8] T. Nakano, Y. Okaie, and A. V. Vasilakos, "Transmission rate control for molecular communication among biological nanomachines," *IEEE Journal of Selected Areas in Communication (JSAC)*, vol. 31, no. 12, pp. 835–846, 2013.
- [9] M. Femminella, G. Reali, and A. V. Vasilakos, "A molecular communications model for drug delivery," *IEEE Transactions on Nanobioscience*, vol. 14, no. 8, pp. 935–945, 2015.
- [10] Y. Okaie, T. Nakano, T. Hara, T. Obuchi, K. Hosoda, Y. Hiraoka, and S. Nishio, "Cooperative target tracking by a mobile bionanosensor network," *IEEE Transactions on Nanobioscience*, vol. 13, no. 3, pp. 267–277, 2014.
- [11] Y. Chen, P. Kosmas, P. S. Anwar, and L. Huang, "A touch-communication framework for drug delivery based on a transient microbot system," *IEEE Transactions on NanoBioscience*, vol. 14, no. 4, pp. 397–408, 2015.
- [12] Y. Okaie, T. Nakano, T. Hara, and S. Nishio, "Autonomous mobile bionanosensor networks for target tracking: A two-dimensional model," *Nano Communication Networks*, vol. 5, no. 3, pp. 63–71, September 2014.
- [13] T. Obuchi, Y. Okaie, T. Nakano, T. Hara, and S. Nishio, "Inbody mobile bionanosensor networks through non-diffusion-based molecular communication," in *Proc. 2015 IEEE Conference on Communications (ICC)*, 2015, pp. 1078–1084.
- [14] T. Nakano, T. Suda, Y. Okaie, M. J. Moore, and A. V. Vasilakos, "Molecular communication among biological nanomachines: A layered architecture and research issues," *IEEE Transactions on Nanobioscience*, 2014.
- [15] T. Nakano, S. Kobayashi, T. Suda, Y. Okaie, Y. Hiraoka, and T. Haraguchi, "Externally controllable molecular communication," *IEEE Journal of Selected Areas in Communication (JSAC)*, vol. 32, no. 12, pp. 2417–2431, 2014.
- [16] L. Lamalice, F. L. Boeuf, and J. Huot, "Endothelial cell migration during angiogenesis," *Circulation Research*, vol. 100, pp. 782–794, 2007.
- [17] J. T. Smith, J. K. Tomfohr, M. C. Wells, T. P. Beebe, Jr., T. B. Kepler, and W. M. Reichert, "Measurement of cell migration on surface-bound fibronectin gradients," *Langmuir*, vol. 20, pp. 8279–8286, 2004.
- [18] J. T. Smith, J. T. Elkin, and W. M. Reichert, "Directed cell migration on fibronectin gradients: effect of gradient slope," *Experimental Cell Research*, vol. 312, no. 13, pp. 2424–2432, 2006.